Flow Reversal of Unsteady Oscillatory Flow in Combined Convection Fully Developed Vertical Channel

Nur Asiah Mohd Makhatar[1,*], Habibis Saleh[2], Farris Aiman Fadzil[1], Ahmad Shahrulazhar Jamali[1], Nurul Hafizah Zainal Abidin[3], Nur Ardiana Amirsom[1]

[1] Mathematical Sciences Studies, College of Computing, Informatics and Mathematics, Bangunan Al-Khawarizmi, Universiti Teknologi MARA, 40450 Shah Alam, Selangor, Malaysia
[2] Department of Mathematics, University of Riau, 28293, Pekanbaru, Indonesia
[3] Mathematical Sciences Studies, College of Computing, Informatics and Mathematics, Universiti Teknologi MARA, Perak Branch, Tapah Campus, 35400 Tapah Road, Perak Darul Ridzuan, Malaysia

ARTICLE INFO

ABSTRACT

Numerical simulations of flow and heat transfer in an unsteady oscillatory fully developed combined convection are conducted. The temperature on the right wall varies with sinusoidal rhythm over time within a locked mean temperature, whereas the temperature on the left wall remains constant. Both walls are also considered to be stationary. A numerical solution for the momentum and energy equations obtained using the Runga- Kutta method is used to analyze the effect of periodic oscillation on the velocity and temperature configurations, as well as the progression of heat generations. The combined convection process of heat transfer and its flow pattern in a vertical channel is important in many applications, including environmental, industrial, and engineering. This study is prompted by a problem with the heat transfer process, which is difficult, expensive, and time-consuming. The purpose of this study is to develop a mathematical model, find a numerical solution, and conduct parametric studies on the double-diffusive fully developed vertical channel with unsteady oscillatory flow, as well as to investigate the effect of various parameters on the velocity and temperature profiles. The effect of different dimensional parameters is tested and the flow reversal phenomenon is discussed. The dimensional equations are transformed into non-dimensional equations using the similarity technique. Then, the built-in program *dsolve* in Maple is used to numerically solve the boundary value problem (BVP). A validation study is conducted on a previously reported problem to confirm the validity of the present calculation. The flow and temperature numerical findings are represented visually. It is found that a large development of flow is caused by the plate temperature oscillation with high amplitude, therefore, the nature of the flow differs from the non-oscillating case.

* Corresponding author.
E-mail address: nur_asiah@tmsk.uitm.edu.my (Nur Asiah Mohd Makhatar)

1. Introduction

Vertical channels play a pivotal role in numerous engineering systems, offering a unique environment for heat transfer studies due to their distinctive flow characteristics. Unlike horizontal channels, vertical channels are subject to gravitational effects that significantly impact fluid dynamics and heat transfer patterns. The convective heat transfer in such channels is influenced by buoyancy forces, generating a complex interplay between conduction, convection, and radiation. The purpose of this research is to comprehensively explore the heat transfer behavior in a fully developed vertical channel. A fully developed flow implies that the velocity profile remains constant along the flow direction, allowing a focused analysis of the heat transfer mechanisms at a specific stage of flow development.

The study of flow reversal in combined convective flow has received much of attention since it was discovered. Sparrow *et al.,* [1] demonstrated reverse flow in an experimental setting. An approximation analysis for parallel-streamline, bidirectional shear flow in combined convection was provided by Najam *et al.,* [2], Raptis and Perdius [3], and Cebeci *et al.,* [4]. For developing and completely developed flow, Aung and Worku [5] offered an analytical solution for combined convection flow in a vertical channel with asymmetric heating of the walls. The investigation of exact solution analysis is critical for determining the accuracy, continuity, and convergence of various numerical computation methods. With regards to double-diffusive convection, among the studies conducted is the one by Salah El-Din [6]. A more recent study, carried out by Hussein [7] revealed that varying the diffusivity ratio of heat, the different molecular diffusivities affect the scalar fluxes through the system. Meanwhile, Legare *et al.,* [8] applied differential diffusion which allows for novel types of hydrodynamic instability to have finite amplitude manifestations even in millimeter-scale channels in their studies.

Many studies have been carried out involving combined convection on a fully developed vertical channel with varying wall temperatures. Among others, works by Jha *et al.,* [9], Jha and Ajibade [10] as well as Lin *et al.,* [11] have been considered. According to Tao [12], the heat transfer problems of combined convection can be expressed in the complex domain as a Helmholtz wave equation. Hamadah and Wirtz [13] use the Darcian force, buoyancy force, and no-slip wall effect to calculate the non-dimensional temperature distribution, heat transfer rate per unit length between two walls, heat managed by fluid, friction coefficient, velocity distribution, and mass flow rates. Some of the earliest systematic research of combined convection in a vertical heated channel was done by Aung *et al.,* [14] and Incropera *et al.,* [15]. Umavathi *et al.,* [16] studied numerically the unsteady flow and heat transfer in a horizontal channel and found that raising the thermal conductivity ratio lowers temperature rise. Later, Umavathi and Shekar [17] investigated the unsteady combined convection flow in a long vertical channel including a porous and fluid layer, which was surrounded by a smooth and corrugated wall. It was discovered that the Grashof number, width ratio, and conductivity ratio all contribute to the promotion of velocity parallel to the flow direction. Some of the more recent studies were carried out by Debnath *et al.,* [18] in which a steady fully developed flow of cohesionless granular materials through a vertical channel is investigated.

In recent years and decades, there has been a great deal of heat transfer and fluid flow research in horizontal or vertical channel involving free, forced, or combined convection, works by Quntiere and Muller [19], Pop *et al.,* [20] as well as Jayabalan *et al.,* [21]. When natural convection and forced convection mechanisms work together to transfer heat, this is referred to as combined forced convection and natural convection. This also refers to situations in which both pressure and buoyant forces interact. Liu *et al.,* [22] mentioned that enhancing heat transfer for more efficient energy utilization is an efficient way to save energy. Conduction, convection, and radiation are the

three heat transfer modes. Heat transfer enhancement or augmentation refers to techniques that contribute positively to an increase in heat transfer coefficient. On a vertical channel, the internal flow can be either upwards or downwards. Some important works on heat transfer in channels using combined convection have been published. The problems have been expanded to include those with linearly varying as well as continuous wall temperature gradients due to certain engineering applications in nuclear reactors, heat exchangers, and so on. These studies are then extended by Bentoto *et al.,* [23], where mixed convection of a MHD oscillatory laminar flow of a nanofluid (Gold-Kerosene oil) in a vertical channel is investigated. It is found that nanofluids have a clear influence on the velocity and temperature behavior. Moreover, the presence of thermal radiation improves the heat transfer rate.

This research on the flow reversal of unsteady oscillatory flow within a combined convection fully developed vertical channel addresses a notable gap in the existing understanding of heat transfer dynamics. While extensive research has individually explored heat transfer in vertical channels and unsteady flows, the specific combination of unsteady oscillatory flow and combined convection in fully developed vertical channels remains relatively underexplored. Existing literature predominantly concentrates on steady-state flow conditions, often neglecting the intricate interactions in fully developed vertical channels. This gap signifies a lack of comprehensive knowledge regarding the occurrence, mechanisms, and implications of flow reversal under these specific conditions. Understanding the interplay between unsteady oscillatory flow, buoyancy forces, and convective heat transfer in fully developed vertical channels is crucial for optimizing thermal performance in diverse engineering applications. Addressing this problem is vital for advancing the field, potentially leading to more accurate models, improved design guidelines, and enhanced control strategies for systems involving fully developed vertical channels subjected to unsteady oscillatory flow and combined convection, thus contributing significantly to the overall comprehension of heat transfer phenomena in complex geometries and transient flow regimes in thermal engineering.

Hence, the interaction of combined convection, double diffusivity, and oscillatory transient flow in a fully developed channel must be carried out. The main purpose of the present work is to develop a mathematical model, find numerical solutions, and perform parametric studies to investigate the unsteady oscillatory flow and heat transfer in double-diffusive combined convection fully developed vertical channel. Several different analytical and numerical methods can be used to solve nonlinear systems of ordinary differential equations. In this study, shooting method is applied for solving the flow and temperature distributions using a built-in routine *dsolve* in MAPLE.

2. Mathematical Formulation

Unsteady oscillatory flow in a fully developed combined convection vertical channel with non-uniform internal heating with width L is considered. The schematic diagram of Figure 1 shows that cartesian coordinate system is applied with x–axis is parallel to the gravitational acceleration g, but with opposite direction and y–axis is normal to it. When $y = -L/2$, the temperature is at a constant cold temperature $T = T_1$, while when $y = -L/2$, the temperature varies sinusoidally in time at $T = T_2 + a \sin \omega t$ with $T_1 < T_2$. This means that it oscillates about non−zero temperature T_2. The flow has a constant upward perpendicular velocity, U_0 at the channel opening.
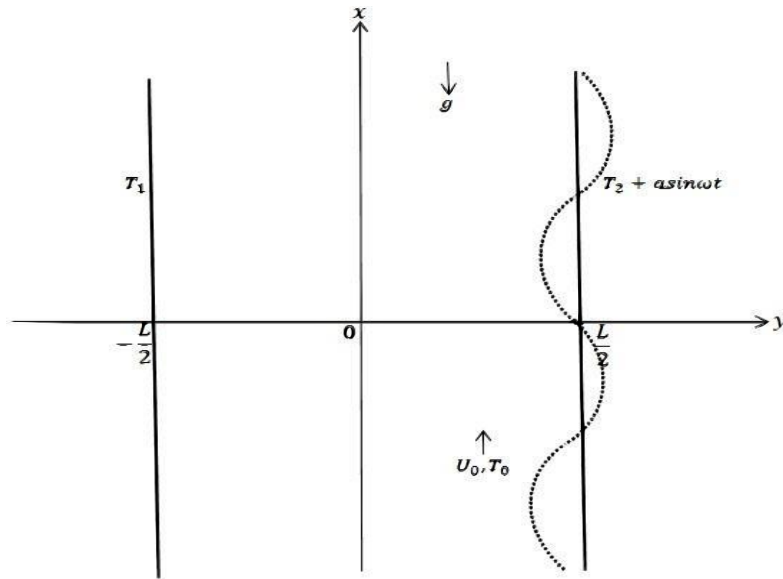
Fig. 1. Physical configuration

The following relations apply if the fully developed assumption is adopted:

$$v = 0, \quad \frac{\partial u}{\partial x} = 0, \quad \frac{\partial T}{\partial x} = 0 \tag{1}$$

$$\frac{\partial p}{\partial y} = 0, \quad \frac{\partial p}{\partial x} = P_x = \text{const}, \tag{2}$$

in which v is the velocity component in y direction and p is the pressure. This will lead to the unsteady flow of the viscous incompressible fluid within this channel under the Boussinesq's approximation which is governed by the following system of partial differential equations:

$$v^2 \frac{\partial u}{\partial t} = v \frac{\partial^2 u}{\partial y^2} + g\beta_T \left(T - T_0\right) + g\beta_c \left(C - C_0\right) - \frac{1}{\rho} \frac{\partial p}{\partial x} \tag{3}$$

$$\frac{\alpha}{v} \frac{\partial T}{\partial t} = \alpha \frac{\partial^2 T}{\partial y^2} + \gamma \left(T - T_1\right)^\lambda \tag{4}$$

with the following boundary conditions:

$$\begin{aligned}
y = -L/2: \quad & u = 0, \quad T = T_1 \\
y = L/2: \quad & u = 0, \quad T = T_2 + a\sin\left(\omega t\right)
\end{aligned} \tag{5}$$

These non−dimensional variables are needed to transform the governing equations into its dimensionless forms:

$$Y = \frac{y}{L}, \quad X = \frac{x}{LRe}, \quad \tau = \frac{tv}{L^2}, \quad U = \frac{u}{u_0}, \quad F = \frac{\omega L^2}{v}, \quad v = \frac{u_0 L}{Re}$$

$$Re = \frac{u_0 l}{v}, \quad G = \frac{\gamma L^2 (\Delta T)^{\lambda-1}}{\alpha}, \quad \theta = \frac{T - T_1}{T_2 - T_1}, \quad GR = \frac{Gr}{Re}, \quad \text{(6)}$$

$$Gr = \frac{g \beta \Delta T L^3}{v^2}, \quad A = \frac{a_1}{T_2 - T_1}, \quad \Delta T = T_2 - T_1$$

Hence, these are the dimensionless forms of the governing equations:

$$\frac{\partial U}{\partial \tau} = GR\theta + \frac{\partial^2 U}{\partial Y^2} - P_x \qquad (7)$$

$$\frac{\partial \theta}{\partial \tau} = \frac{\partial^2 \theta}{\partial Y^2} + G\theta^\lambda \qquad (8)$$

and the corresponding boundary conditions are

$$\begin{aligned} Y = -1/4: \quad U = 0, \quad \theta = 0 \\ Y = -1/4: \quad U = 0, \quad \theta = 1 + A\sin(F\tau) \end{aligned} \qquad (9)$$

where U is the dimensionless velocity, θ is the dimensionless fluid temperature, F is the dimensionless frequency of the oscillations of the plate temperature, GR is the dimensionless combined convection parameter and A is the unit of energy used to describe waves.

In justifying the numerical code, it is important to carry out a similarity test with the previous related studies. The current numerical outputs will be compared to the output acquired by Barletta [24]. Considering the effect of viscosity dissipation, Barletta [24] conducted an analytical study on combined, free, and forced convection flow in a parallel plate vertical channel in the fully developed region. According to the study, viscous dissipation increases the effect of flow reversal in the case of downward flow while decreasing this effect in the case of upward flow. Viscous dissipation also increases the buoyancy force.

Grid independence study was also carried out as in Figure 2. The effect of grid resolution was examined in order to select the appropriate grid density.
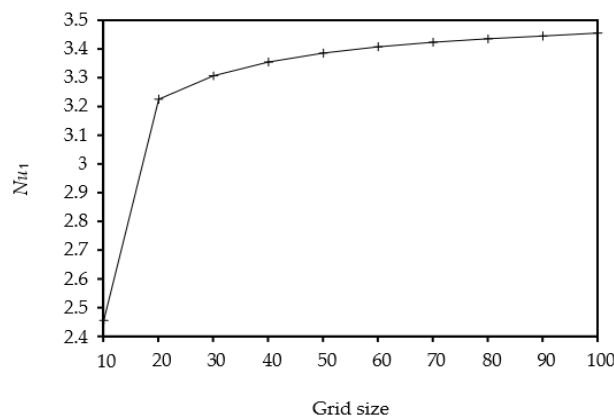
Fig. 2. Grid independence study

The numerical computing is done using MAPLE, a fourth-generation programming language created by MathWorks. Maple is available in many operating system such as Windows, Linux, and Mac Os. Partial differential equations (PDEs) and the systems of PDEs are solved using the MAPLE *pdsolve* code. The main objective of the *pdsolve* function is to find an analytical solution. Despite the type, differential order, or quantity of dependent or independent variables in the systems, *pdsolve* would be able to solve PDEs or PDE systems. For now, only certain PDE groups that could be solved with common approach are acknowledged by *pdsolve* command. If the PDE originates from a group that the *pdsolve* command does not recognize, a heuristic algorithm that separates the variables in accordance with the PDE's structure is used. The purpose of *pdsolve* was to produce the PDE's most typical solution or just to separate the variables.

3. Results and Discussions

A comparison with a previously published result is required to validate the numerical code. The numerical results are compared to the obtained results by Barletta [24], which is shown in Figure 3 (a) for GR=0. Based on this comparison, the current results as shown in Figure 3(b), agree perfectly with the corresponding result by Barletta [24].

3.1 Velocity and Temperature Profiles

The foregoing problem indicates that flow reversal of unsteady oscillatory flow in combined convection fully developed double diffusive vertical channel which is governed by six nondimensional parameters in the domain: Combined convection parameter $150 \leq GR \leq 300$, dimensionless time $0.1 \leq \tau \leq 0.4$, amplitude $0.1 \leq A \leq 0.5$, frequency $10\pi \leq F \leq 55\pi$, internal heat generation $0 \leq G \leq 70$ and local heating exponent $1 \leq \lambda \leq 4$.

(a)

(b)
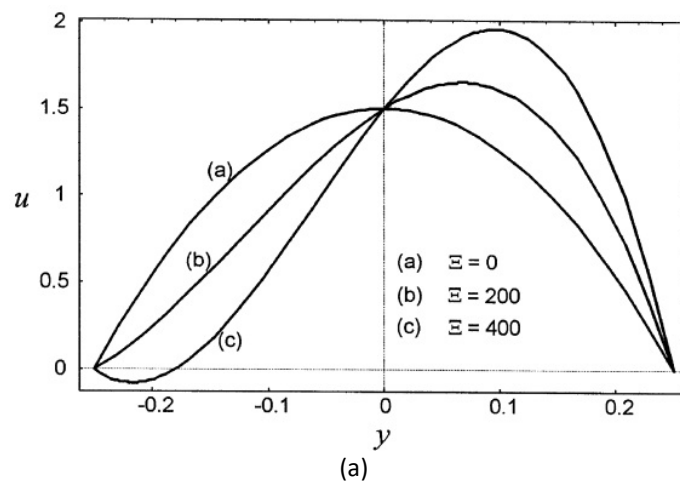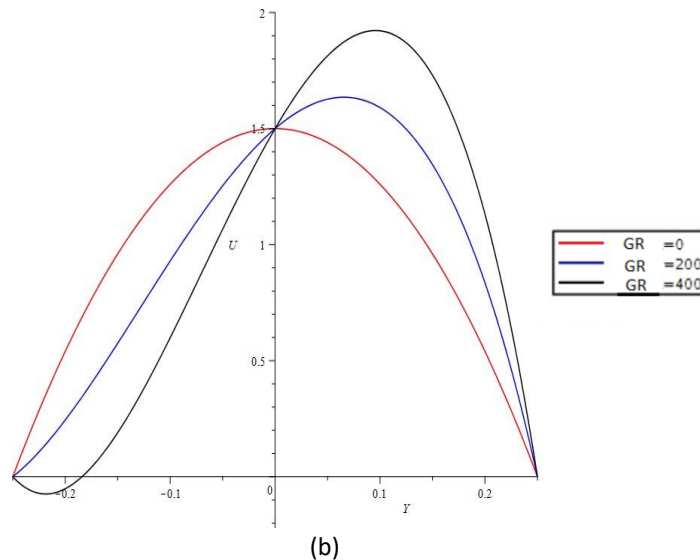
Fig. 3. Velocity configurations of (a) Barletta [24] and (b) current research for different combined convection parameter *GR* with *G* = 0, *A* = 0, F = 10π, τ = 2.0 and λ = 1

The velocity profile in Figure 4 shows the influence of GR. It reflects that the effect of GR is more significant on the left wall. As the value of GR increases, the flow rate decreases. At GR = 200, there is still no sight of reversal flow in the channel. However, As GR > 250, the reversal flow of velocity profile starts to occur. This is because as GR increases, wall heating becomes sufficiently intense and may cause reversal flow in buoyancy-assisted flow. The higher combined convection parameter leads to a strong distortion of the velocity configurations affected by the presence of strong reverse flow. These velocity profiles are highly unstable, hence inducing significant fluctuations. Meanwhile, with regards to the temperature profile as shown in Figure 5, different variations of GR did not change the temperature profile. It demonstrates that the impact of GR on the temperature profile becomes negligible as the value of GR increases.
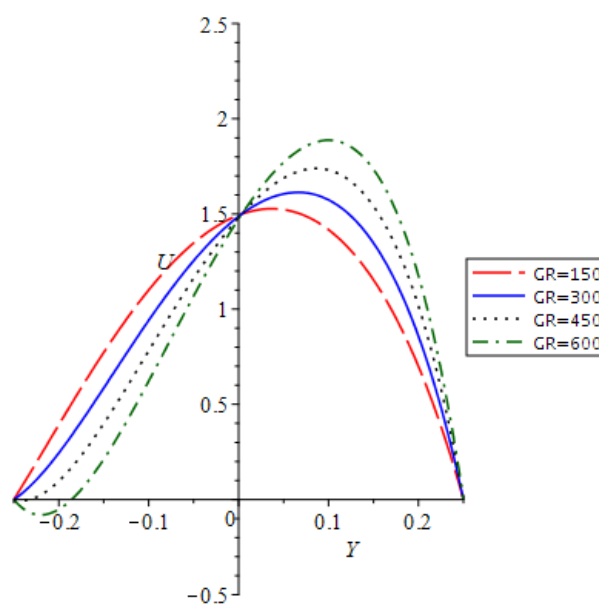
Fig. 4. Velocity profile of varied Combined Convection Parameter (GR)
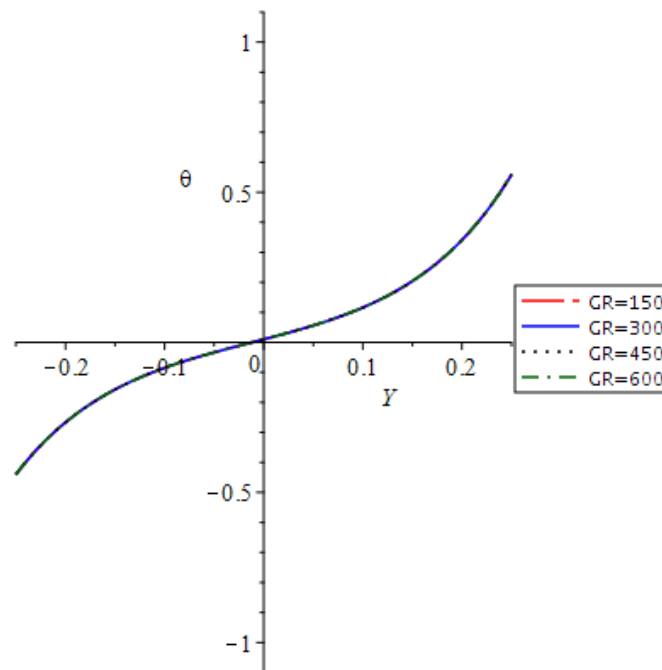
Fig. 5. Temperature profile of varied Combined Convection Parameter (GR)

Figure 6 and Figure 7 show the effects of different values of τ respectively on the velocity and temperature profiles. In the velocity profile, as τ increases, the fluid velocity decreases near the cold wall and gradually increases as it approaches the right wall. Flow reversal started to appear as τ >0.03. With reference to the temperature profile in Figure 7, initially, the temperature on the left wall is higher than the temperature of the fluid inside the channel. As the temperature on the left wall rises, the temperature of fluid particles near the left wall rises because the left wall transmits heat. As time passes, heat moves from the left wall to the mid-channel and then to the right wall. As a result, as τ increases, the temperature distribution will have a linear profile and will eventually become steady.
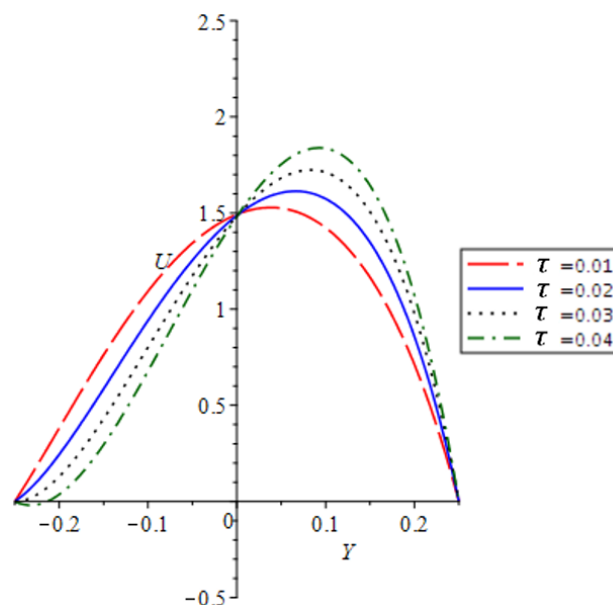
Fig. 6. Velocity profile of varied Dimensionless Time (τ)
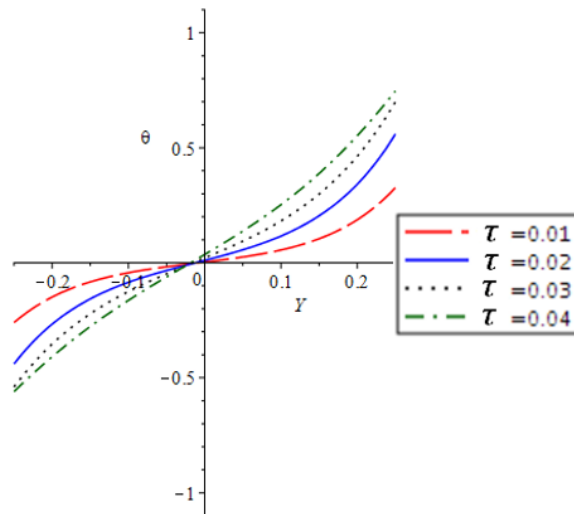
Fig. 7. Temperature profile of varied dimensionless time (τ)

Figure 8 represents the velocity profile of varied A, resulting a positive skewness. The positive skewness in this case occurs due to the sinusoidal heating on the right wall. The peak of heating in the velocity profile reaches when value Y between 0.1 and 0.2. It is also noticed that the reversal flow started to occur when A>0.3. With regards to the temperature profile in Figure 9, the temperature does not show a significant difference with the increased value of A, however, the temperature shows a prominent increase with the increase of A when the velocity approaches the right wall.
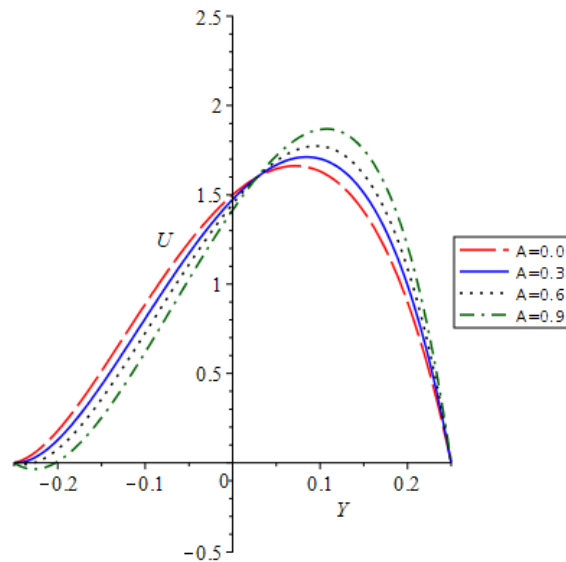
Fig. 8. Velocity profile of varied Amplitude (A)
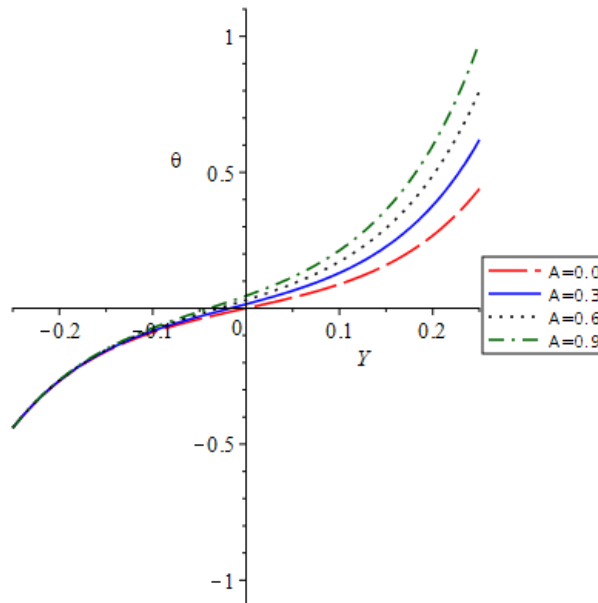
Fig. 9. Temperature profile of varied Amplitude (A)

The velocity profile of varied F in Figure 10 shows an increase of the velocity with the increase of F from the left wall until mid-channel. However, the velocity decreases with the increase of F from mid-channel towards the right wall. The velocity profile reaches its heating peak when value Y between 0.1 and 0.2. The reversal flow appears for the value $F>20\pi$. Figure 11 shows that as the value F increases, the temperature profile decreases and demonstrates substantial variation on the right wall since the temperature on the left wall is constant while the temperature on the right channel varies sinusoidally in time.
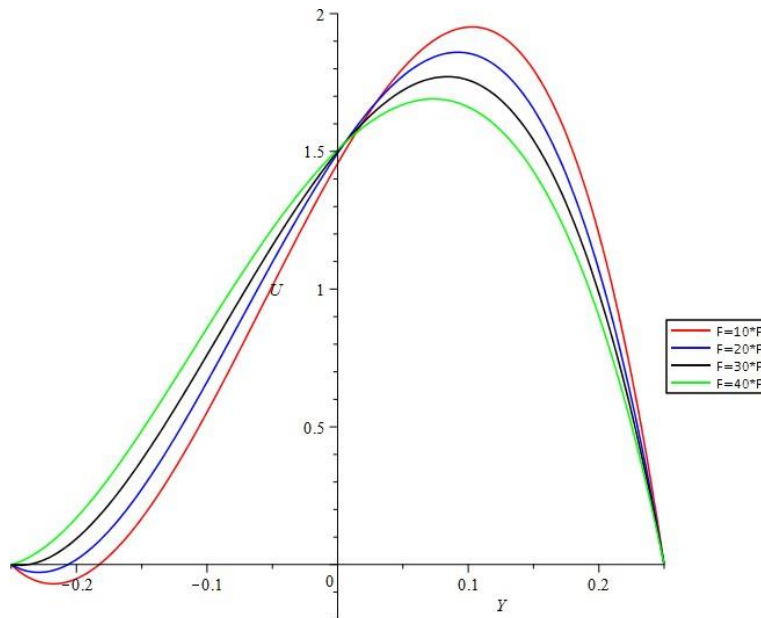
Fig. 10. Velocity profile of varied Frequency (F)
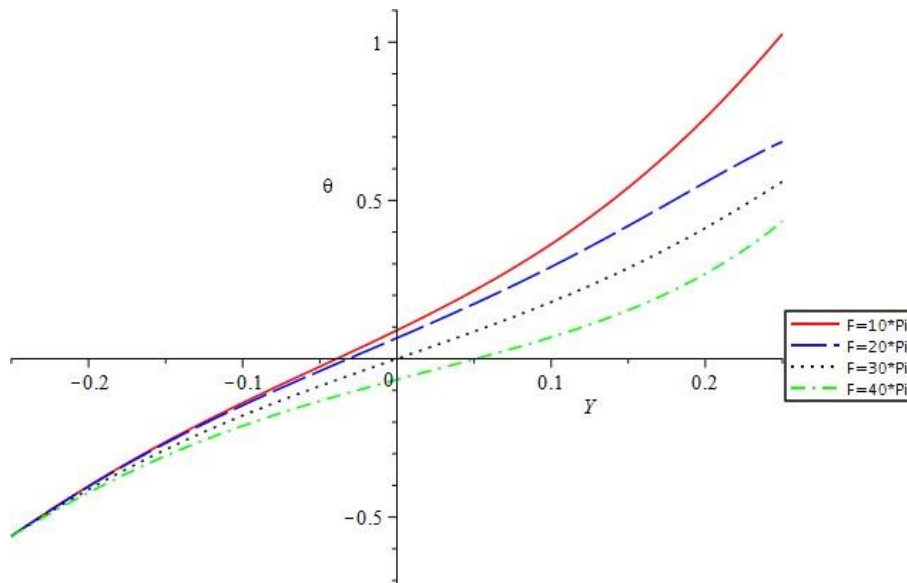
Fig. 11. Temperature profile of varied Frequency (F)

It is important to note that the negative signs in G figures are solely used to distinguish between heat transfer and heat absorption conditions. Fluid heating is associated with a negative value of G, whereas fluid cooling is associated with a positive value of G. With reference to Figure 12, as the value of G increases, the velocity increases on the right side of the wall while decreases on the left side. According to the graph, flow reversal occurs since G ≥ 0 and close to the right wall. Meanwhile, in Figure 13, the temperature distribution is linear when G ≤ 50. When the value of G is increases, the temperature on the right side of the wall rises, while the temperature on the left side of the wall rises slightly. Increasing G causes the fluid to heat up, transferring heat from the centre of the channel to the warmer channel wall.
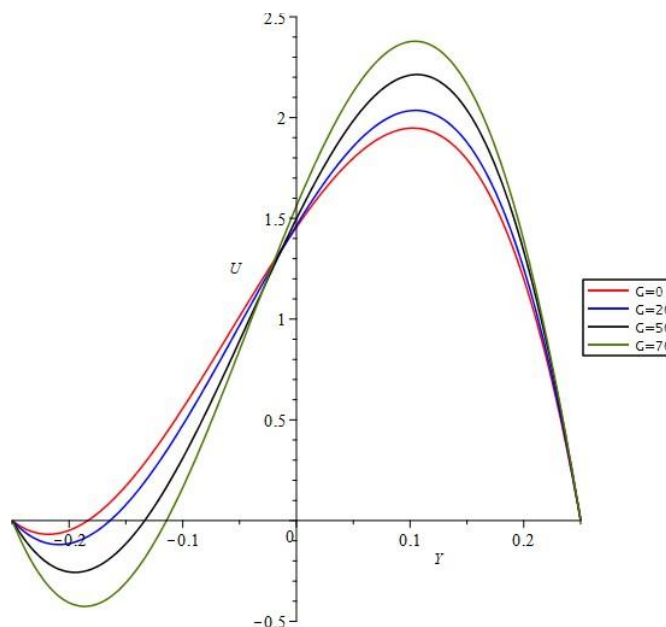
Fig. 12. Velocity profile of varied Internal Heat Generation (G)
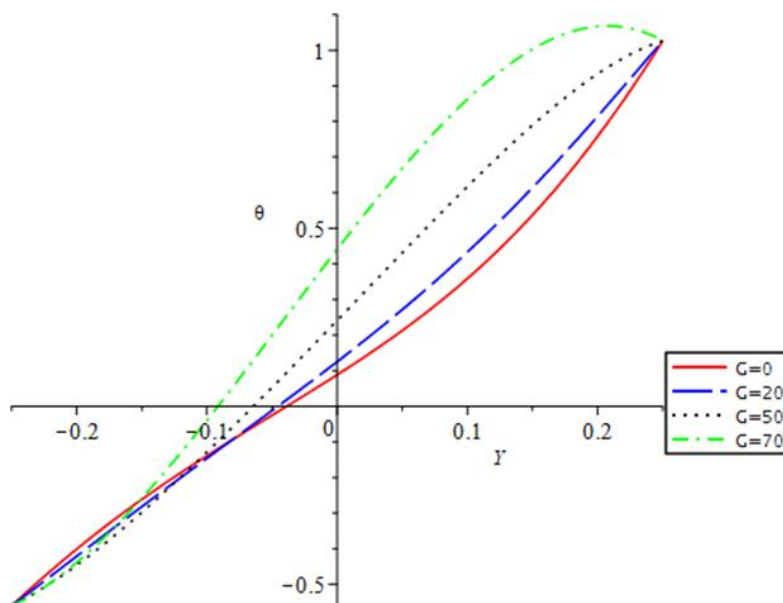
Fig. 13. Temperature profile of Internal Heat Generation (G)

Figure 14 represents the effects of various p values on the velocity profiles. As p increases, the dimensionless velocity increases from the left wall to the channel's centre and decreases from the centre to the right wall. The flow reversal occurs for all values of p, and the velocity distribution is skewed towards the right wall. It can also be demonstrated that as p increases, the effect of p on the design velocity shrinks. Because the G value is more dominant than the p value, the velocity profile does not show significant changes in flow design as p increases. Figure 15 illustrates the effects of various p values on temperature profiles. As shown in the figures, the dimensionless temperature rises from the colder wall to the channel's centre. The flow design looks similar when p is varied. It is also demonstrated that as p increases, p does not give any significant effect on the temperature profile.
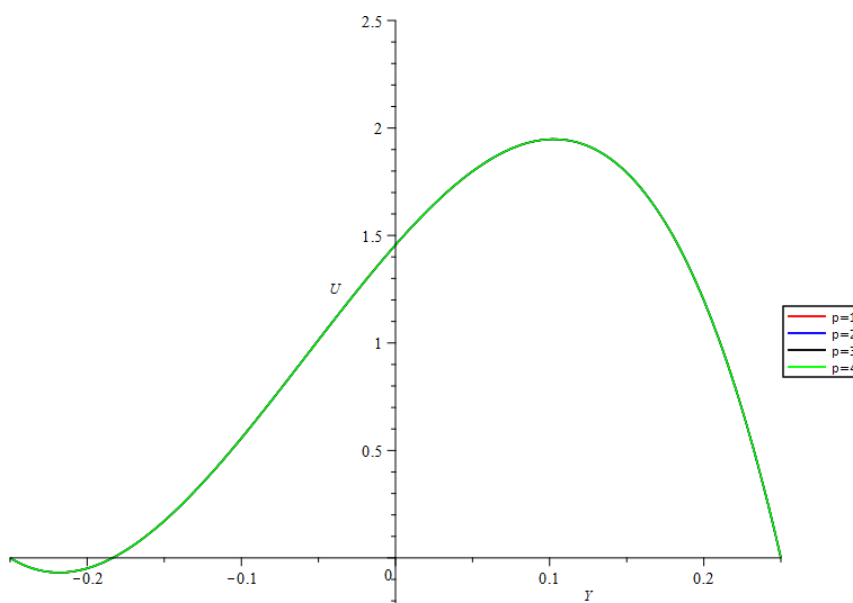
Fig. 14. Velocity profile of varied Local Heat Exponent (p)
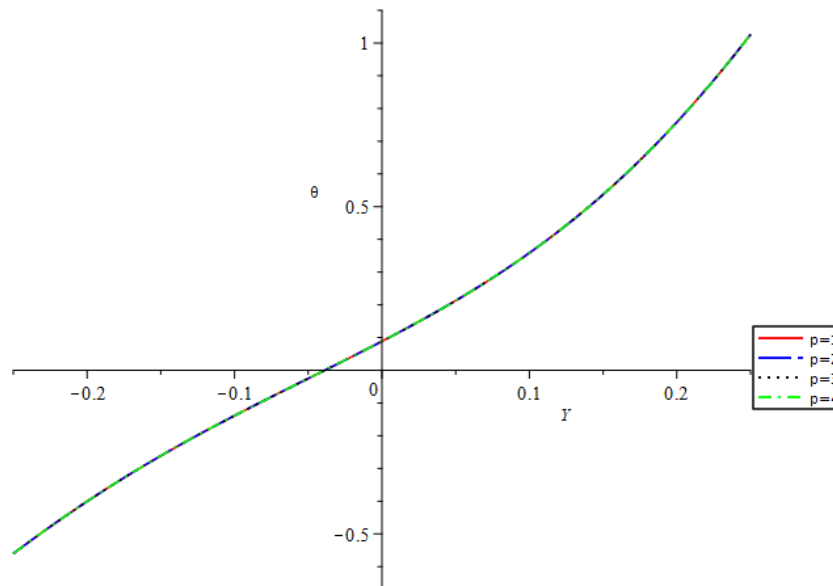
Fig. 15. Temperature profile of varied Local Heat Exponent (p)

3.2 Heat Transfer Evaluation

In thermal system design, it is vital to have the outcomes for diversities in time of the local Nusselt number over the heated part at the channel sides for different parameters. Nusselt number *Nu* symbolizes the heat transfer rate with Nu_1 representing the colder wall and Nu_2 is the hotter wall. Heat-transfer movement at the hotter wall is from the channel wall to the fluid when $Nu_2 > 0$, meanwhile when $Nu_2 < 0$, heat-transfer movement at the hotter wall is from the fluid to the channel wall. Similarly, heat-transfer direction at the colder wall is from the liquid to the wall when $Nu_1 > 0$, and heat-transfer direction at the colder wall is from the wall to the liquid when $Nu_1 < 0$. Figures 16–18 represents a more detailed discussions on flow asymmetry and oscillation of the time traces for Nusselt numbers on the left wall Nu_1 and right wall Nu_2. For all the cases, since temperature on the left channel is constant whereas temperature on the right channel varies sinusoidally in time, the magnitude of oscillation is more severe for the graphs of Nusselt numbers on the right wall Nu_2.

Figures 16(a) and 16(b) represents the diversity of Nusselt numbers, Nu1 and Nu2 respectively for different values of A at GR = 200, G = 5, Ω = 10π and λ = 2. The heat transfer rate oscillates with increasing periodic variation for Nu1 and decreasing periodic variation for Nu2 of the source temperature signal for all amplitudes examined in this study. The plate temperature oscillation with large amplitude resulted a significant amplification of flow, hence, the instantaneous of the flow differs much from the non-oscillating case. These affects yield wider fluctuating of the Nusselt numbers when A takes larger values and this is more obvious for the case of Nu2. The instantaneous values of Nu1 reach a sharp negative values when τ = 0.1 before making a sharp oscillatory increase between 0.1 ≤ τ ≤ 0.2. The perfectly increasing sinusoidal functions for Nu1 appears when τ ≥ 0.3. Meanwhile, Nu2 makes a perfectly decreasing sinusoidal laws for all A values when τ ≥ 0.1.
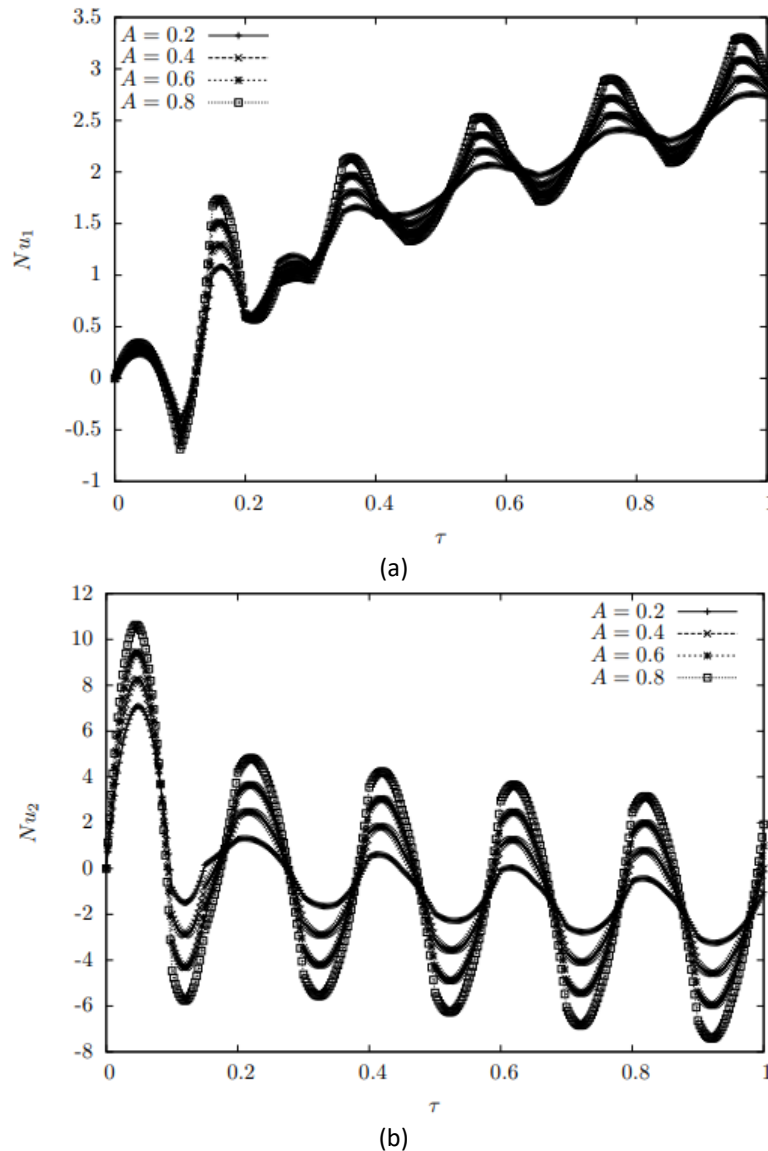
Fig. 16. Variation of the Nusselt numbers (a) Nu_1 and (b) Nu_2
for varied values of A with G = 5, GR = 200, Ω = 10π and p = 2

The variation of Nusselt numbers Nu_1 and Nu_2 with varied values of Ω at GR = 200, G = 5, A = 0.6 and p = 2 is depicted in Figures 17(a) and 17(b). Increasing sinusoidal function is clearly seen around τ > 0.3 for Nu_1 and τ > 0.2 for Nu_2. After τ = 0.1, the heat generations both for Nu_1 and Nu_2 are not stable when Ω = 2π and Ω = 20π. They abruptly became rather insignificant after the fluctuations are initiated. The oscillatory heat transfer for both walls generally have the highest amplitude when Ω = 15π. These fluctuating heat transfer characteristics show that at this condition, the momentum and convective flow slows down with slight modification in repetition of the thermal frequency. Meanwhile, the right wall shows an opposite nature with decreasing sinusoidal function.
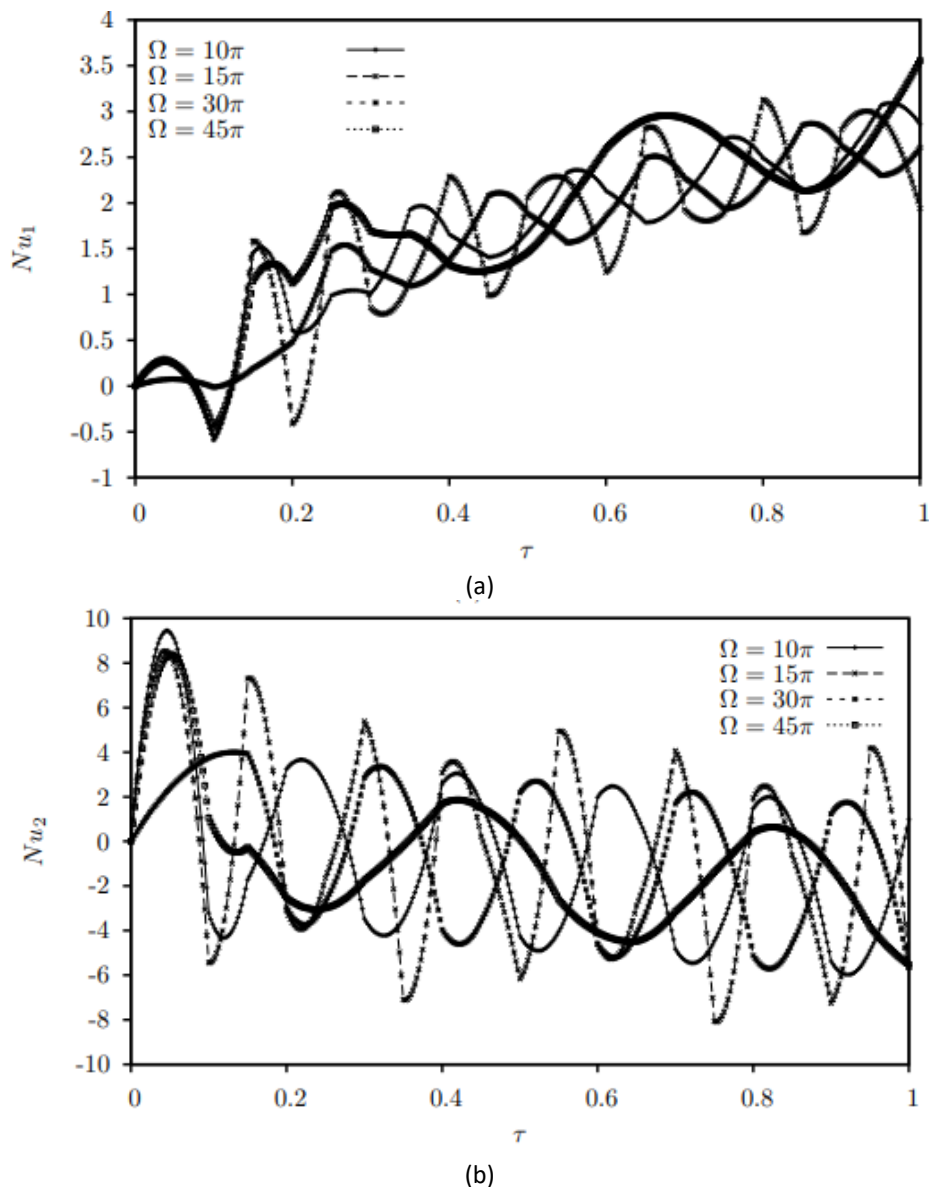
Fig. 17. Variation of the Nusselt numbers (a) Nu_1 and (b) Nu_2 for varied values of Ω with $G = 5$, $A = 0.6$, $GR = 200$ and p = 2

Figure 18 displays the time traces of the Nusselt numbers for various values of G at τ = 0.04, GR = 200, $A = 0.6$, $\Omega = 10\pi$ and p = 2. The heat transfer on the left wall Nu_1 increases with the increase of G. Meanwhile, the heat transfer on the right wall Nu_2 is seen to decrease with the increase of G. This is because since the oscillatory temperature occurs on the right wall, it reduces the temperature difference between the fluid and the channel. The result also reveals that for Nu_1, the heat transfer formed a sinusoidal function around $\tau > 0.3$ for Nu_1 and $\tau > 0.1$ for Nu_2. However, with high values of G ($G > 6$), Nu_1 deviate and do not follow sinusoidal function. Meanwhile, when $G > 6$, Nu_2 is still sinusoidal but the fluctuation is more extreme.

(a)

(b)
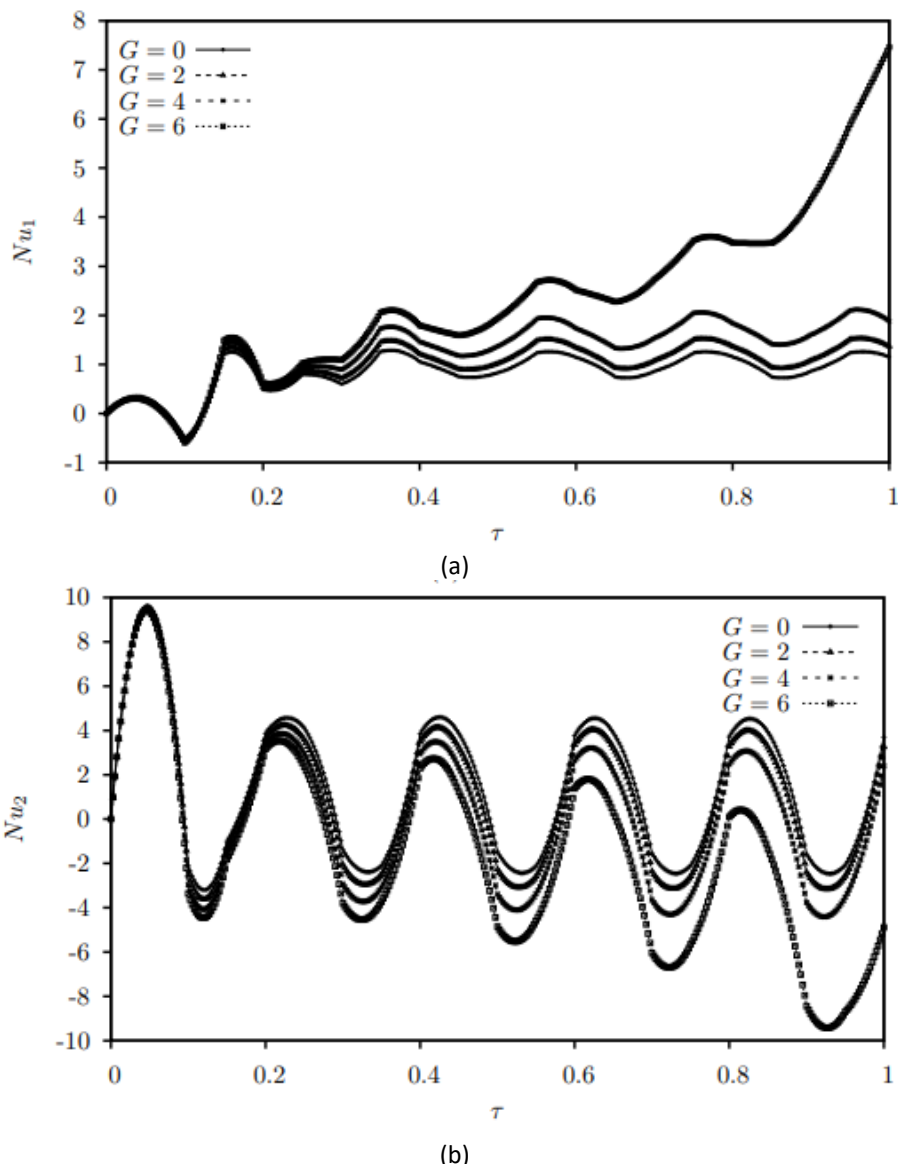
Fig. 18. Variation of the Nusselt numbers (a) Nu_1 and (b) Nu_2 for varied values of G with GR = 200, A = 0.6, Ω = 10π and p =2

Tables 1 and 2 respectively show time−integrated Nusselt number at Y = −0.25 (Nu_1) and Y = 0.25 (Nu_2) for various combination of G, F and A when p = 2, λ = 200. The time-integrated Nusselt number are defined as $\int_0^\tau Nu_1 \, d\tau$ and $\int_0^\tau Nu_2 \, d\tau$. Nu_1 increases by increasing G value while Nu_2 decreases by increasing G value. A higher value of A brings more enhancement in Nu_1 for the considered F while a higher value of A brings more reduction in Nu_2 for the considered F. Finally, the time-integrated Nu_1 and Nu_2 can be correlated well with the value of A and F as a function of G as below:

$$\overline{Nu_1} = \left[0.68 + \frac{A}{0.7}\right] - \frac{0.1}{\sqrt[7]{F}}\left(1 - e^{-\left[0.33 + \frac{A}{0.7}\right]G}\right)$$

$$\overline{Nu_2} = \left[1.75 + \frac{A}{7}\right] + \frac{0.3 + 2A}{\sqrt[4]{F}}\left(1 - e^{-\left[0.33 + \frac{A}{7}\right]G}\right) \tag{10}$$

Table 1

Time–average Nusselt number at $Y = -\frac{1}{2}\ \overline{Nu_1}$ for various combination of *G*, *F* and *A* at *p* = 2, GR = 200

	$F = \dfrac{5}{\pi}$		$F = \dfrac{15}{\pi}$	
G	*A* = 0.4	*A* = 0.8	*A* = 0.4	*A* = 0.8
1.0	0.767213	0.803607	0.746275	0.758205
1.5	0.795691	0.836856	0.772677	0.784751
2.0	0.827802	0.874983	0.80227	0.81454
2.5	0.86431	0.91915	0.835697	0.848229
3.0	0.906236	0.970965	0.87381	0.88669
3.5	0.954988	1.032746	0.917766	0.931111
4.0	1.012578	1.107996	0.969194	0.983168
4.5	1.082034	1.20285	1.030484	1.04533
5.0	1.168204	1.325984	1.105351	1.121447
5.5	1.279592	1.499463	1.200027	1.218019
6.0	1.433357	1.778094	1.326226	1.347372

Table 2

Time–average Nusselt number at $Y = -\frac{1}{2}\ \overline{Nu_2}$ for various combination of *G*, *F* and *A* at *p* = 2, GR = 200

	$F = \dfrac{5}{\pi}$		$F = \dfrac{15}{\pi}$	
G	*A* = 0.4	*A* = 0.8	*A* = 0.4	*A* = 0.8
1.0	1.607137	1.749728	1.609534	1.773717
1.5	1.487965	1.601537	1.506535	1.669328
2.0	1.360689	1.442236	1.396705	1.558001
2.5	1.223887	1.269686	1.278868	1.438538
3.0	1.075681	1.080983	1.151496	1.309375
3.5	0.913524	0.872024	1.012538	1.168411
4.0	0.733811	0.636692	0.859146	1.012722
4.5	0.531192	0.365216	0.687201	0.838064
5.0	0.297181	0.040367	0.49039	0.637902
5.5	0.017029	-0.37312	0.258275	0.401366
6.0	-0.3387	-0.96927	-0.02845	0.108144

4. Conclusions

This study focuses on unsteady fully developed oscillatory flow in combined convection vertical channel with non-uniform internal heating. The main results are as follows:

1. The higher combined convection parameter leads to a strong distortion of the velocity configurations affected by the presence of strong reverse flow. These velocity profiles are highly unstable, hence inducing significant fluctuations.
2. Increasing both dimensionless amplitude and oscillation frequency shows an obvious rise in the velocity profiles in the right portion, while a clear reduction is observed in the left portion of the channel.
3. In general, since the temperature on the left channel is constant whereas the temperature on the right channel varies sinusoidally in time, the magnitude of oscillation is more severe for the graphs of Nusselt numbers on the right wall.

4. It is found that a large development of flow is caused by the plate temperature oscillation with high amplitude, therefore, the nature of the flow differs from the non-oscillating case. As a result; A wider fluctuating of the Nusselt numbers for higher amplitude values and this is more obvious at the right wall.

5. The oscillatory heat transfer for both walls generally has the highest amplitude at relatively low oscillating frequency. In such a condition, the momentum and convective flow slow down with slight modification in repetition of the thermal frequency.

The heat transfer process of combined convection and its flow pattern in a vertical channel is important, especially in environmental, industrial and engineering applications. These results would help to overcome the concern regarding the heat transfer process in which it is difficult, expensive and time consuming.

Acknowledgement

References

[1] Sparrow, E. M., G. M. Chrysler, and L. F. Azevedo. "Observed flow reversals and measured-predicted Nusselt numbers for natural convection in a one-sided heated vertical channel." (1984): 325-332. https://doi.org/10.1115/1.3246676

[2] Najam, M., A. Amahmid, M. Hasnaoui, and M. El Alami. "Unsteady mixed convection in a horizontal channel with rectangular blocks periodically distributed on its lower wall." *International Journal of Heat and Fluid Flow* 24, no. 5 (2003): 726-735. https://doi.org/10.1016/S0142-727X(03)00063-8

[3] Raptis, A. A., and C. P. Perdikis. "Oscillatory flow through a porous medium by the presence of free convective flow." *International journal of engineering science* 23, no. 1 (1985): 51-55. https://doi.org/10.1016/0020-7225(85)90015-1

[4] Cebeci, Tuncer, A. A. Khattab, and R. LaMont. "Combined natural and forced convection in vertical ducts." In *International Heat Transfer Conference Digital Library*. Begel House Inc., 1982. https://doi.org/10.1615/IHTC7.2840

[5] Aung, Win, and G. Worku. "Developing flow and flow reversal in a vertical channel with asymmetric wall temperatures." (1986): 299-304. https://doi.org/10.1115/1.3246919

[6] El-Din, MM Salah. "Fully developed forced convection in a vertical channel with combined buoyancy forces." *International communications in heat and mass transfer* 19, no. 2 (1992): 239-248. https://doi.org/10.1016/0735-1933(92)90035-G

[7] Hussein, Sameh A. "Numerical simulation for peristaltic transport of radiative and dissipative MHD Prandtl nanofluid through the vertical asymmetric channel in the presence of double diffusion convection." *Numerical Heat Transfer, Part B: Fundamentals* (2023): 1-27. https://doi.org/10.48550/arXiv.2207.09230

[8] Legare, Sierra, Andrew Grace, and Marek Stastna. "Double diffusive instability with a constriction." *Physics of Fluids* 35, no. 2 (2023). https://doi.org/10.1063/5.0135159

[9] Jha, Basant K., Abiodun O. Ajibade, and Deborah Daramola. "Mixed convection flow in a vertical tube filled with porous material with time-periodic boundary condition: steady-periodic regime." *Afrika Matematika* 26, no. 3-4 (2015): 529-543. https://doi.org/10.1007/s13370-013-0222-y

[10] Jha, Basant K., and Abiodun O. Ajibade. "Free convective flow of heat generating/absorbing fluid between vertical porous plates with periodic heat input." *International communications in heat and mass transfer* 36, no. 6 (2009): 624-631. https://doi.org/10.1016/j.icheatmasstransfer.2009.03.003

[11] Lin, Tsing-Fa, Tsai-Shou Chang, and Yu-Feng Chen. "Development of oscillatory asymmetric recirculating flow in transient laminar opposing mixed convection in a symmetrically heated vertical channel." (1993): 342-352. https://doi.org/10.1115/1.2910685

[12] Tao, L. N. "On combined free and forced convection in channels." (1960): 233-238. https://doi.org/10.1115/1.3679915

[13] Hamadah, T. T., and R. A. Wirtz. "Analysis of laminar fully developed mixed convection in a vertical channel with opposing buoyancy." *Journal of Heat Transfer (Transactions of the ASME (American Society of Mechanical Engineers), Series C);(United States)* 113, no. 2 (1991). https://doi.org/10.1115/1.2910593

[14] Aung, W. "Mixed convection in internal flow." *Handbook of single-phase convective heat transfer* 15 (1987).

[15] Incropera, Frank P. "Buoyancy effects in double-diffusive and mixed convection flows." In *International Heat Transfer Conference Digital Library*. Begel House Inc., 1986. https://doi.org/10.1615/IHTC8.2340

[16] Umavathi, Jawali C., Ali J. Chamkha, Abdul Mateen, and Ali Al-Mudhaf. "Unsteady two-fluid flow and heat transfer in a horizontal channel." *Heat and Mass Transfer* 42, no. 2 (2005): 81-90. https://doi.org/10.1007/s00231-004-0565-x

[17] Umavathi, Jawali C., and Marudappa Shekar. "Unsteady mixed convective flow confined between vertical wavy wall and parallel flat wall filled with porous and fluid layer." *Heat Transfer Engineering* 36, no. 1 (2015): 1-20. https://doi.org/10.1080/01457632.2014.897576

[18] Debnath, Bhanjan, V. Kumaran, and K. Kesava Rao. "Comparison of the compressible μ (I) class of models and non-local models with the discrete element method (DEM) for steady fully developed flow of cohesionless granular materials through a vertical channel–CORRIGENDUM." *Journal of Fluid Mechanics* 955 (2023): E1. https://doi.org/10.1017/jfm.2022.1006

[19] Quintiere, J., and W. K. Mueller. "An analysis of laminar free and forced convection between finite vertical parallel plates." (1973): 53-59. https://doi.org/10.1115/1.3450004

[20] Pop, Ioan, Teodor Grosan, and Revnic Cornelia. "Effect of heat generated by an exothermic reaction on the fully developed mixed convection flow in a vertical channel." *Communications in Nonlinear Science and Numerical Simulation* 15, no. 3 (2010): 471-474. https://doi.org/10.1016/j.cnsns.2009.04.010

[21] Jayabalan, C., K. K. Sivagnana Prabhu, and R. Kandasamy. "Heat enhanced by an exothermic reaction on a fully developed MHD mixed convection flow in a vertical channel." *Journal of Applied Mechanics and Technical Physics* 57 (2016): 957-962. https://doi.org/10.1134/S0021894416050242

[22] Liu, W., P. Liu, J. B. Wang, N. B. Zheng, and Z. C. Liu. "Exergy destruction minimization: A principle to convective heat transfer enhancement." *International Journal of Heat and Mass Transfer* 122 (2018): 11-21. https://doi.org/10.1016/j.ijheatmasstransfer.2018.01.048

[23] Bentoto, W., M. Zaydan, H. Amini Alaoui, E. Essaghir, and R. Sehaqui. "Mixed convection of a MHD oscillatory laminar flow of a nanofluid (Gold-Kerosene oil) in a vertical channel." *Statistics, Optimization & Information Computing* 11, no. 1 (2023): 55-69. https://doi.org/10.19139/soic-2310-5070-1725

[24] Barletta, Antonio. "Laminar mixed convection with viscous dissipation in a vertical channel." *International Journal of Heat and Mass Transfer* 41, no. 22 (1998): 3501-3513. https://doi.org/10.1016/S0017-9310(98)00074-X